DOI: 10.1002/chem.200800670

Hydrogen Bonds as Structural Directive towards Unusual Polynuclear Complexes: Synthesis, Structure, and Magnetic Properties of Copper(II) and Nickel(II) Complexes with a 2-Aminoglucose Ligand

Anja Burkhardt, Eike T. Spielberg, Sascha Simon, Helmar Görls, Axel Buchholz, and Winfried Plass*[a]

Abstract: The reaction of benzyl 2-amino-4,6-*O*-benzylidene-2-deoxy-α-D-glucopyranoside (HL) with the metal salts $Cu(ClO_4)_2 \cdot 6H_2O$ and $Ni(NO_3)_2 \cdot 6H_2O$ affords via self-assembly a tetranuclear μ_4-hydroxido bridged copper(II) complex $[(\mu_4\text{-}OH)Cu_4(L)_4(MeOH)_3(H_2O)](ClO_4)_3$ (**1**) and a trinuclear alcoholate bridged nickel(II) complex $[Ni_3(L)_5(HL)]NO_3$ (**2**), respectively. Both complexes crystallize in the acentric space group $P2_1$. The X-ray crystal structure reveals the rare $(\mu_4\text{-}OH)Cu_4O_4$ core for complex **1** which is μ_2-alcoholate bridged. The copper(II) ions possess a distorted square-pyramidal geometry with an $[NO_4]$ donor set. The core is stabilized by hydrogen bonding between the coordinating amino group of the glucose backbone and the benzylidene protected oxygen atom O4 of a neighboring {Cu(L)} fragment as hydrogen-bond acceptor. For complex **2** an $[N_4O_2]$ donor set is observed at the nickel(II) ions with a distorted octahedral geometry. The trinuclear isosceles Ni_3 core is bridged by μ_3-alcoholate O3 oxygen atoms of two glucose ligands. The two short edges are capped by μ_2-alcoholate O3 oxygen atoms of the two ligands coordinated at the nickel(II) ion at the vertex of these two edges. Along the elongated edge of the triangle a strong hydrogen bond (244 pm) between the O3 oxygen atoms of ligands coordinating at the two relevant nickel(II) ions is observed. The coordinating amino groups of the these two glucose ligands are involved in additional hydrogen bonds with O4 oxygen atoms of adjacent ligands further stabilizing the trinuclear core. The carbohydrate backbones in all cases adopt the stable $^4C_1$ chair conformation and exhibit the rare chitosan-like *trans*-2,3-chelation. Temperature dependent magnetic measurements indicate an overall antiferromagnetic behavior for complex **1** with $J_1 = -260$ and $J_2 = -205\ cm^{-1}$ ($g = 2.122$). Compound **2** is the first ferromagnetically coupled trinuclear nickel(II) complex with $J_A = 16.4$ and $J_B = 11.0\ cm^{-1}$ ($g_{1,2} = 2.183$, $g_3 = 2.247$). For the high-spin nickel(II) centers a zero-field splitting of $D_{1,2} = 3.7\ cm^{-1}$ and $D_3 = 1.8\ cm^{-1}$ is observed. The $S = 3$ ground state of complex **2** is consistent with magnetization measurements at low temperatures.

Keywords: carbohydrates · copper · hydrogen bonds · magnetic properties · nickel

Introduction

Carbohydrates are the most abundant biogenic class of compounds involved in a wide range of functions in living organisms, for example, monosaccharide fragments are participating in glycolipids and glycoproteins.[1] Many sugar-metabolizing enzymes have been revealed to function with alkaline earth and transition-metal ions in the active sites.[2] Although the importance of sugar–metal interaction has been known for many years,[3] information on the metal-binding of saccharide moieties is still rather limited. Only for the past two decades, sugars received a growing interest as ligand components in coordination chemistry because of their stable chiral scaffold, supramolecular arrangement via hydrogen bonding, and polyfunctionality.[3,4] In particular the latter aspect is of interest related to the field of high-nuclearity transition-metal complexes which have been attracting continuous interest due to their relevance for multimetal active sites of metalloproteins[5] as well as their importance in the field of molecular magnetism.[6]

[a] Dr. A. Burkhardt, E. T. Spielberg, S. Simon, Dr. H. Görls, Dr. A. Buchholz, Prof. Dr. W. Plass
Institut für Anorganische und Analytische Chemie
Friedrich-Schiller-Universität Jena, Carl-Zeiss-Promenade 10
07745 Jena (Germany)
Fax: (+49) 3641-948-132
E-mail: sekr.plass@uni-jena.de

From the coordination chemistry point of view, carbohydrates are suitable chelate ligands functionalized with a sequence of weak donor sites. The vicinal functional groups feature several donor atoms capable of forming stable complexes with transition metals[7] and offer several possibilities to introduce additional donor groups into the sugar backbone. Well-known modification strategies are *N*-glycosylation of polyamines[8,9] and nucleophilic substitution of bromoethyl-*O*-glycosides.[10] TEMPO oxidation of the secondary hydroxyl group at C6 results in the formation of uronic acids. The corresponding carbohydrate-derived salicylidene hydrazides are obtained via a three-step synthesis and form mononuclear VO_2^+ complexes.[11] On the other hand, condensation of amino saccharides and carbonyl components readily leads to tridentate Schiff-base ligands.[12,13] These Schiff-base ligands are based on either C1 or C6 amino functionalized carbohydrate fragments.[13] In the case of their copper(II) complexes varying nuclearities and architectures are observed, where the structure of the central Cu_n unit ($n=2,3,4$) can be influenced by the positions of the chelating donor atoms at the sugar backbone. Linear alcoholate–acetate-bridged trinuclear copper(II) compounds were obtained from glucopyranose derivatives carrying an imino- or ketoenamine residue at C6, whereas 5-ketoenamine-substituted glucofuranoses as well as Schiff-base derivatives of 1- or 2-aminoglucopyranoses yield di- or tetranuclear alcoholate-bridged complexes.[14–16]

In this context we started to explore the coordination chemistry of 2-aminoglucopyranoses as chitosan-like chelate ligands.[17–20] In particular, their copper(II) compounds show a considerable tendency to self-aggregate affording oxoido-bridged oligonuclear complexes with unexpected magnetic properties induced by hydrogen bonding between the constituting glucose ligands.[17] The formation of oxygen bridged polynuclear compounds is a general feature for transition-metal complexes with carbohydrate derivatives as ligands,[21,8] which is usually prevented by the presence of appropriate coligands to coordinatively saturate the metal ion. Nevertheless very little is known about relevant carbohydrate-based polynuclear complexes.[22]

Herein we present the synthesis and characterization of polynuclear copper(II) and nickel(II) complexes derived from a 2-aminoglucose ligand with the rare chitosan-like *trans*-2,3-chelation by the sugar backbone. The molecular structures are directed by the possible hydrogen bonding theme given by the ligand system. In the case of copper(II) this leads to a tetranuclear complex with an unusual (μ_4-OH)Cu_4O_4 core, whereas for nickel(II) the rare case of a isosceles triangular Ni_3 core is obtained. To our knowledge, the obtained nickel(II) complex is the first trinuclear example that exhibits ferromagnetic interactions.

Results and Discussion

Synthesis and characterization: The 2-aminoglucose ligand benzyl 2-amino-4,6-*O*-benzylidene-2-deoxy-α-D-glucopyranoside (HL) was obtained in a three-step synthesis according to published procedures starting from *N*-acetyl-α-D-glucopyranosamine as depicted in Scheme 1.[23] In the first two steps the glycosidic hydroxyl group of the anomeric carbon atom C1 and the hydroxyl groups at C4 and C6 are protected as benzyl ether and cyclic benzylidene acetal, respectively. The following alkaline hydrolysis of the amide function at C2 affords the bidentate 2-aminoglucose ligand HL. Due to the hydrophobic character of the phenyl groups HL is soluble in less polar solvents such as chloroform. The exclusive presence of the α-anomer of the saccharide unit, associated with the *cis* position of the protons attached to C1 and C2, is confirmed by the resonance of the proton on C1 of the D-glucose moiety which leads to a doublet with $^3J_{12}=3.7$ Hz in the ^{1}H NMR spectrum of HL.

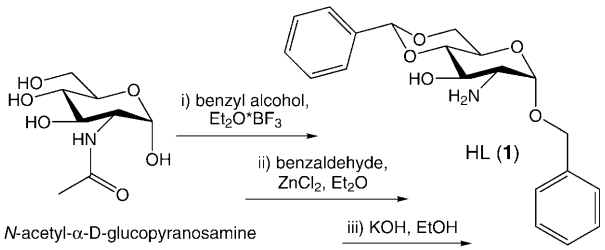

Scheme 1. Synthesis of ligand HL starting from *N*-acetyl-α-D-glucopyranosamine.

For the synthesis of the copper(II) complex a methanol solution of copper(II) perchlorate hexahydrate is treated with a solution of the ligand HL in chloroform in a 1:1 molar ratio at room temperature. Slow evaporation of the solvent leads to blue prismatic crystals [(μ_4-OH)Cu_4(L)$_4$-(MeOH)$_3$(H_2O)](ClO_4)$_3$ (**1**) containing additional solvent molecules of crystallization. This is confirmed by TGA measurements of freshly isolated crystals. Variation of the reaction conditions by addition of a stoichiometric amount of triethylamine leads the same tetranuclear copper(II) complex **1**, but without significant increase in yield. Crystals of better X-ray quality have been obtained by the base-free method. The electronic absorption spectrum of complex **1** in chloroform solution exhibits a charge-transfer band at 278 nm and a d–d transition band at 696 nm. To the best of our knowledge complex **1** is the first tetranuclear copper(II) complex with μ_4-hydroxido bridged Cu_4 core without support of a macrocyclic ligand.[24]

The reaction of nickel(II) nitrate hexahydrate with two equivalents of the 2-aminoglucose ligand HL in methanol solution in the presence of two equivalents of aqueous potassium hydroxide leads to the trinuclear complex [Ni_3(L)$_5$(HL)]NO_3 (**2**). Single crystals containing additional solvent molecules of crystallization which are suitable for X-ray structure analysis could be obtained by slow evaporation of the solvent. This is consistent with the TGA measurements of freshly isolated crystals. The electronic absorption spectrum of complex **2** in chloroform solution shows two

low energy bands at 643 and 1131 nm which are typical for octahedral high-spin nickel(II) ions.[25,26] To our knowledge **2** is the first trinuclear nickel(II) complex based on a carbohydrate ligand system.

Structure description: Crystals of complexes **1** and **2** suitable for X-ray crystallography have been grown by slow evaporation of the employed solvent. For both complexes the obtained crystals contain methanol and water molecules of crystallization which are located on disordered positions. For complexes **1** and **2** this leads to the crystal compositions $[(\mu_4\text{-OH})Cu_4(L)_4(MeOH)_3(H_2O)](ClO_4)_3 \cdot 2.7\,MeOH$ (**1**·2.7 MeOH) and $[Ni_3(L)_5(HL)]NO_3 \cdot 3.25\,MeOH \cdot 0.75\,H_2O$ (**2**·3.25 MeOH·0.75 H_2O), respectively. Both compounds crystallize in the monoclinic space group $P2_1$ consistent with the exclusive presence of one enantiomeric form. Details of the crystal structure determination are summarized in the Experimental Section.

Copper(II) complex 1: The molecular structure of the cation of compound **1** is depicted in Figure 1. Selected bond lengths and angles as well as interatomic distances are listed in Table 1. The tetranuclear copper(II) complex consists of four {Cu(L)} building blocks which are linked by a central μ_4-OH group. All four copper(II) ions possess $[NO_4]$ coordination environments with a slightly distorted square-pyramidal geometry as indicated by the corresponding τ values which range from 0.15 to 0.32 ($\tau = 0$ for a square pyramid, $\tau = 1$ for a trigonal bipyramid).[27] This is in accordance with the small deviations of 17 to 25 pm observed for the copper(II) ions from their basal coordination planes given by the C2 amino nitrogen atom and the C3 alcoholate oxygen atom of the sugar backbone, an additional C3 alcoholate oxygen atom of the ligand of an adjacent {Cu(L)} moiety, and the oxygen atom O1 of the central μ_4-OH bridge. The deprotonated oxygen atoms O*i*3 of the chelating glucose backbone are the μ_2-bridging links between two copper(II) ions (*i* is the running number of the {Cu(L)} fragments). The square planes of the four {Cu(L)} fragments are rotated approximately 90° with respect to their neighbors which are linked by sharing two adjacent edges of the square planes. This is supported by intramolecular hydrogen bonds between the amino nitrogen atom and the oxygen atom at C4 of neighboring {Cu(L)} building blocks. The relevant distances N*i*···O*j*4 vary from 276 to 291 pm (*i* and *j* are the running numbers of the adjacent {Cu(L)} fragments). The glucose backbones of all four {Cu(L)} building blocks adopt the generally more stable $^4C_1$ chair conformation.

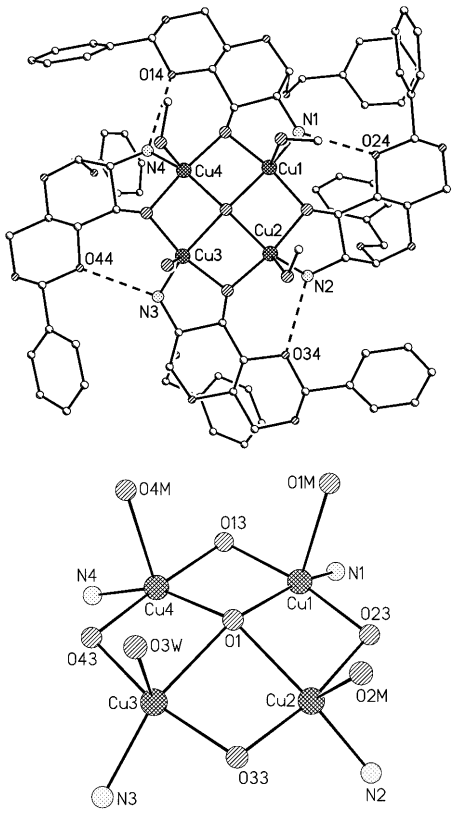

Figure 1. Molecular structure of the cation $[(\mu_4\text{-OH})Cu_4(L)_4(MeOH)_3(H_2O)]^{3+}$ of complex **1**. Solvent molecules, hydrogen atoms, and perchlorate counterions are omitted for clarity. Disordered phenyl rings are displayed in one position. Top: Cation with intramolecular hydrogen bonds indicated by dashed lines. Pertinent distances: N1···O24 291, N2···O34 291, N3···O44 290, N4···O14 276 pm. Bottom: Representation of the tetranuclear μ_4-OH bridged core of **1** with the coordination environment of the copper(II) centers.

Table 1. Selected bond lengths, interatomic distances [pm], and Cu-O-Cu bridging angles [°] for **1**.

Distances			
Cu1–O1	211.8(4)	Cu2–O1	216.0(4)
Cu1–N1	200.5(5)	Cu2–N2	199.6(5)
Cu1–O13	194.0(4)	Cu2–O23	192.9(4)
Cu1–O23	191.2(4)	Cu2–O33	190.5(4)
Cu1–O1M	223.3(4)	Cu2–O2M	217.7(4)
Cu3–O1	221.7(4)	Cu4–O1	211.8(4)
Cu3–N3	201.4(4)	Cu4–N4	199.2(5)
Cu3–O33	190.7(4)	Cu4–O13	191.3(4)
Cu3–O43	189.8(4)	Cu4–O43	192.8(4)
Cu3–O3W	216.2(5)	Cu4–O4M	221.9(5)
Cu1···Cu2	291.68(10)	Cu2···Cu3	295.63(10)
Cu1···Cu3	419.29(14)	Cu2···Cu4	407.67(12)
Cu1···Cu4	290.41(10)	Cu3···Cu4	292.55(10)
Cu-O-Cu bridging angles			
Cu1-O1-Cu2	85.97(14)	Cu2-O1-Cu3	84.97(14)
Cu1-O1-Cu3	150.5(2)	Cu2-O1-Cu4	144.7(2)
Cu1-O1-Cu4	86.55(15)	Cu3-O1-Cu4	84.85(13)
Cu1-O13-Cu4	97.84(17)	Cu2-O33-Cu3	101.69(17)
Cu1-O23-Cu2	98.80(16)	Cu3-O43-Cu4	99.74(17)

The slight variation in the coordination geometry of the copper(II) ions in the four {Cu(L)} building blocks can be attributed to differences in their axial coordination. The apical position at Cu1, Cu2, and Cu4 is occupied by a methanol molecule. Whereas in the case of Cu3 a water molecule is axially bound to the metal center. All bond lengths and angles of complex **1** are in the expected range. The overall charge of the complex cation $[(\mu_4\text{-OH})Cu_4(L)_4(MeOH)_3(H_2O)]^{3+}$ is consistent with the perchlorate counterions pres-

ent. Except for Cl2P (see Figure 2), the perchlorate ions are highly disordered at several crystallographic positions. Nevertheless, the actual protonation of the central bridging oxygen atom O1 and the axial oxygen ligands at the copper(II) ions can not be directly determined by X-ray crystallography. We therefore performed bond-valence sum (BVS) calculations[28] to confirm both the overall charge of the complex cation and the protonation state of the oxygen atoms coordinated at the copper ions. The corresponding data are given in Table 2.

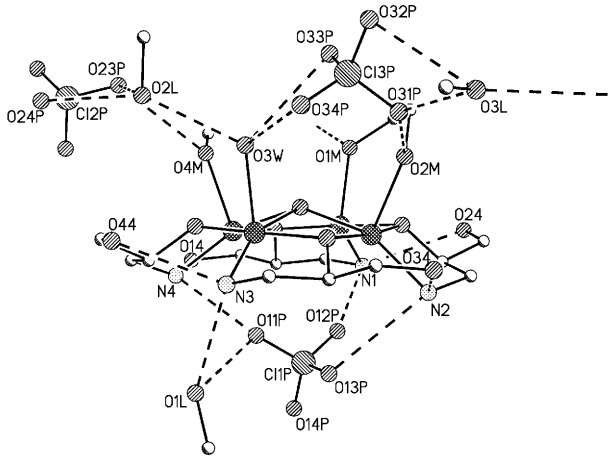

Figure 2. Hydrogen bonding for **1**·2.7 MeOH. All atoms of the complex cation except those involved in hydrogen bonding, coordinated to copper(II), and the carbon atoms of the carbohydrate backbone chelate rings are omitted for clarity. Hydrogen bonds are represented as dashed lines. Pertinent distances: O1M···O3LA 268, O2M···O41P 282, O3W···O2L 272, O3W···O33P 323, O3W···O34P 314, O4M···O23P 303, N1···O24 291, N1···O12P 301, N2···O13P 317, N2···O24 291, N3···O1L 300, N3···O44 290, N4···O11P 305, N4···O14 276, O1L···O11P 279, O2L···O23P 307, O2L···O24P 309, O3L···O31P 282, O3L···O32P 299 pm.

Table 2. BVS values for selected atoms in the crystal structure of **1**; values including hydrogen atoms at preset distances used in the solution of the crystal structure are given in parentheses.[a]

O1	1.12 (2.12)	N1	1.35 (3.25)
O3W	0.27 (2.12)	N2	1.31 (3.20)
O1M	1.18 (2.18)	N3	1.36 (3.25)
O2M	1.10 (2.10)	N4	1.38 (3.28)
O4M	1.23 (2.23)	Cu1	1.90
O13	1.95	Cu2	1.94
O23	1.96	Cu3	1.93
O33	1.99	Cu4	1.94
O43	1.96		

[a] BVS values are calculated according to reference [28]. BVS = $\Sigma_i \exp[(r_{0,i}-r_i)/B]$ with $B = 37$ pm, $r_{0,Cu-O} = 167.9$ pm, $r_{0,Cu-N} = 161.0$ pm, $r_{0,C-O} = 139.0$ pm, $r_{0,C-N} = 147.0$ pm, $r_{0,O-H} = 95.0$ pm, and $r_{0,N-H} = 90.0$ pm.

The BVS values for the central copper(II) ions as well as the μ_2-bridging alkoxido oxygen atoms O*i*3 are in good agreement with the expected value of two. As the hydrogen atoms in the crystal structure of **1** could not be found and refined, the primarily obtained BVS values correspond to a non-protonated situation. In the case of the amine nitrogen atoms N*i* the inclusion of the attached hydrogen atoms at their preset distances, as used in the crystal structure solution, gives values in good agreement with their trivalent character. A similar situation is observed for the axially coordinated oxygen atoms at the copper(II) ions, for which the primarily obtained BVS values clearly indicate that an additional protonation is present. This is consistent with three methanol (O1M, O2M, and O4M) and one water molecule (O3W). Also for central μ_4-bridging oxygen atom the primarily obtained BVS value clearly indicates the presence of an additional proton leading to a hydroxido group at O1, which is consistent with an electron density picks in the difference Fourier map, even though a hydrogen atom could not be refinement at this position. The consequently pentacoordinated oxygen atom O1 of the central μ_4-bridging hydroxido group is displaced by 59 pm from the mean plane defined by the four copper(II) ions located at the corners of the basal plane of the square-pyramidal coordination environment.

The μ_4-OH bridge observed in complex **1** is a rare structural feature, which to the best of our knowledge thus far has solely been reported for complexes with Robson-type macrocyclic ligands.[24] The majority of μ_4-oxygen bridged copper(II) complexes contain a central oxoido group with a tetrahedral coordination sphere.[29] Nevertheless, the by far more common structural motif for tetranuclear copper(II) compounds is a cubane-like Cu_4O_4 core,[30] which thus far has been exclusively observed in the case of complexes with sugar-based ligands.[15–18]

The crystal structure of **1**·2.7 MeOH is characterized by extensive hydrogen bonding and intermolecular π–π interaction of the benzyl substituents at the C1 position. The hydrogen bonding associated with the cation $[(\mu_4\text{-OH})Cu_4(L)_4(MeOH)_3(H_2O)]^{3+}$ of complex **1** is depicted in Figure 2. The interactions of the axial ligands at the copper(II) ions together with two of the perchlorate counterions, one of which is highly disordered (Cl3P) and solvent molecules lead to a hydrogen-bonding network forming one-dimensional chains with a two-fold screw symmetry along the crystallographic [010] direction. The third perchlorate ion is located on two disordered positions in the cavity below the Cu_4 plane of the complex cation, opposite to the central μ_4-OH group O1. This cavity is surrounded by the benzyl groups of the glucose fragments and provides additional space for a methanol molecule (O1L) besides the disordered perchlorate ion.

Nickel(II) complex 2: Figure 3 shows the molecular structure of the cation $[Ni_3(L)_5(HL)]^+$ of complex **2**, which is present in crystals of **2**·3.25 MeOH·0.75 H_2O. Selected bond lengths and the Ni-O-Ni bridging angles are summarized in Table 3. The $[N_2O_4]$ donor set provided by the chelating 2-aminoglucose ligands leads to a distorted octahedral coordination geometry for all three nickel(II) ions. The distortion from the ideal octahedral geometry is best described by the observed bite angles of the chelate ligands ranging from 81 to 85° and the *trans* angles at the nickel(II) centers of 154 to

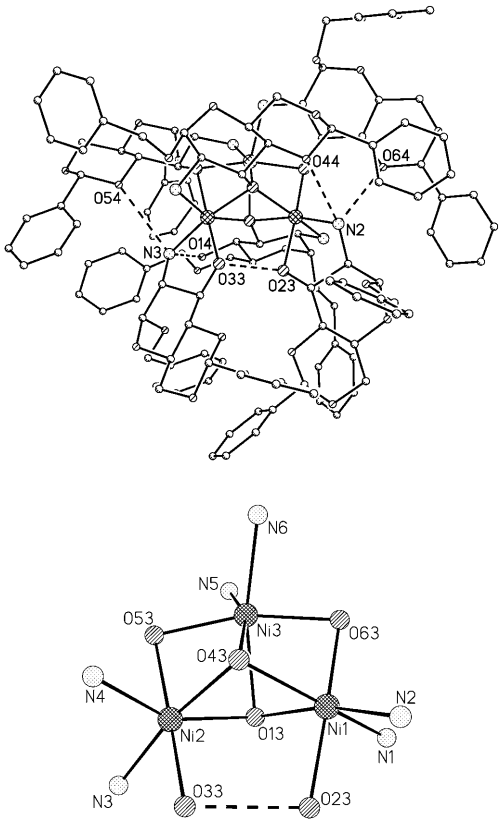

Figure 3. Molecular structure of the cation $[Ni_3(L)_5(HL)]^+$ of complex **2**. Solvent molecules, hydrogen atoms, and the nitrate counterion are omitted for clarity. Disordered phenyl rings are displayed in one position. Top: Cation with intramolecular hydrogen bonds indicated by dashed lines. Pertinent distances: N2···O44 302, N2···O64 307, N3···O14 297, N3···O54 316, O23···O33 244 pm. Bottom: Representation of the trinuclear core of **2** with the coordination environment of the nickel(II) centers.

Table 3. Selected bond lengths, interatomic distances [pm], and Ni-O-Ni bridging angles [°] for **2**.

Distances			
Ni1−N1	209.4(4)	Ni1−O23	205.2(3)
Ni1−N2	212.1(3)	Ni1−O43	209.6(3)
Ni1−O13	210.3(3)	Ni1−O63	201.9(3)
Ni2−N3	209.1(3)	Ni2−O33	208.5(3)
Ni2−N4	211.0(3)	Ni2−O43	208.0(2)
Ni2−O13	212.6(2)	Ni2−O53	205.6(3)
Ni3−N5	216.1(3)	Ni3−O43	222.2(3)
Ni3−N6	214.1(3)	Ni3−O53	198.0(3)
Ni3−O13	218.2(3)	Ni3−O63	199.1(3)
Ni1···Ni3	280.41(7)	Ni2···Ni3	283.36(7)
Ni1···Ni2	316.36(7)		
Ni-O-Ni bridging angles			
Ni1-O13-Ni2	96.83(10)	Ni1-O63-Ni3	88.74(9)
Ni1-O13-Ni3	81.73(8)	Ni2-O13-Ni3	82.25(10)
Ni1-O43-Ni2	98.48(10)	Ni2-O43-Ni3	82.32(10)
Ni1-O43-Ni3	80.92(8)	Ni2-O53-Ni3	89.16(11)

172°. Overall the most significant distortion is observed for the nickel center Ni3. Nevertheless, all bond lengths and angles of complex **2** are within the expected range.

The nickel(II) ions of the trinuclear complex **2** are arranged as nearly isosceles triangle with two almost equivalent Ni···Ni distances of 280 (Ni1···Ni2) and 283 pm (Ni2···Ni3), and one elongated basal edge with 316 pm (Ni1···Ni2). The isosceles triangle formed by the Ni_3 core is μ_3-bridged by the alcoholate O3 oxygen atoms of two 2-aminoglucose ligands coordinated to the nickel centers Ni1 and Ni2. These μ_3-bridging oxygen atoms (O13 and O43) are located about 127 pm above and below the Ni_3 plane. Along the equal sides of the isosceles triangle the nickel ions are additionally linked by μ_2-bridging O3 oxygen atoms of two ligand molecules coordinated to Ni3. This leads to a face sharing of the central octahedron (Ni3) with the two terminal octahedra (Ni1 and Ni2) and an edge sharing between the two latter. Overall each nickel(II) ion is coordinated by two bidentate ligand moieties through the C2 amino nitrogen atom and the C3 alcoholic oxygen atom of the glucose backbone. Consequently, Ni1 and Ni2 are both coordinated by an additional chelating ligand which is not involved in any bridging of metal ions with the oxygen atoms O23 and O33 terminally bound to Ni1 and Ni2, respectively. The carbohydrate backbones of all 2-aminoglucose ligands adopt the stable $^4C_1$ chair conformation.

Along the elongated basal edge of the isosceles triangle a strong hydrogen bond with an O23···O33 separation of 244 pm is formed between the O3 oxygen atoms terminally bound to Ni1 and Ni2 (see Figure 3). A somewhat larger distance is observed for a trinuclear nickel complex with a comparable core structure supported by a methanol–phenolate interaction at a separation of 255 pm.[31] Nevertheless, comparably short oxygen atom distances at about 244 pm are also observed for hydrogen bonds between metal bound alcohol and alcoholate groups (M-(R)O···H-O(R)-M) in copper(II) complexes with amino alcohol ligands.[32] Additional intramolecular hydrogen bonding is observed for the amino nitrogen atoms N2 and N3 of the two terminally bound chelate ligands at Ni1 and Ni2, respectively. These nitrogen atoms form hydrogen bonds with the O4 oxygen atoms of the remaining four 2-aminoglucose ligands with distances in the range of 302 to 316 pm, further stabilizing the trinuclear core (see Figure 3).

Trinuclear nickel(II) complexes with a Ni_3 core motif similar to that of complex **2** have been reported for phenolate bridges between the nickel(II) atoms.[33] Moreover, this structural motif has also been found for a hexanuclear nickel(II) complex with an amino alcohol ligand.[34] Although in particular the coordination chemistry of *N*-glycosylamine ligands has been extensively studied in the past,[3,35] to our knowledge complex **2** is the first trinuclear nickel(II) compound based on a carbohydrate ligand system.

Structural directives in complexes with 2-aminoglucose ligands: For the copper(II) and nickel(II) complexes **1** and **2** unusual structures have been obtained. This can be attributed to the specific properties of the employed 2-aminoglucose ligand HL, which leads to a controlled self-assembly of the basic mononuclear building blocks {Cu(L)} and {Ni(L)$_2$}.

It is well-known that in particular polynuclear copper(II) complexes are governed by the presence of a Cu_4O_4 core. Compounds with such a core structure have been classified according their atomic distances within the core structure as depicted in Figure 4.[30,36] Nearly all structures reported to date fall into two classes, which are characterized according their number of short and long Cu···Cu distances within the Cu_4O_4 core as 2 + 4 class (or type I) and 4 + 2 class (or type II) (see Figure 4), with the latter being by far the more common of the two cases.

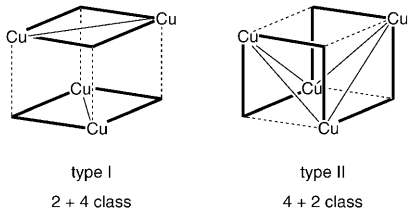

Figure 4. Tetranuclear cubane-like copper(II) complexes classified according their Cu–O and Cu···Cu distances of the Cu_4O_4 core. Thick lines represent short and dashed lines long Cu–O distances. Short Cu···Cu distances are indicated by a connecting line.

Utilizing the *trans*-2,3-chelating glucose backbone as chelating amino alcohol ligand to set up the mononuclear building blocks we have been able to selectively generate examples of either of the two major cubane classes as depicted in Figure 5. The variation of the substitution at the C2 and C3 positions of the glucose backbone can be used to introduce a specific coordinative and supramolecular presetting.

For a 2-aminoglucose imino functionalized at the C2 position and C4/C6 protected by a cyclic benzylidene acetal a 4 + 2 class core structure is obtained.[18] This can be rationalized by the possible weak coordination of the O4 oxygen atom which is in an ideal position, due to the planarity of the tridentate Schiff-base ligand and the rigidity of the glucose backbone. This interaction is favored with respect to the competing one with the μ_2-bridging C3 alkoxide oxygen atom. Due to the lack of appropriate donors, the O4 oxygen atom can not undergo any kind of hydrogen-bonding interaction.

On the other hand using the same ligand, but without protecting group at the O4 oxygen atom, this particular function becomes a potential hydrogen-bond donor. Consequently, the resulting building block is capable of self-aggregation through hydrogen bonding. Instead of the competing situation as in the former case, the hydrogen-bonding interactions of the O4 hydroxy groups synergistically enforce the formation of the μ_3 bridges of the relevant C3 alkoxide oxygen atoms. As a result a 2 + 4 class core structure is obtained.[17]

If the protecting group at O4 is retained, but instead a free 2-amino function is employed, the bidentate amino alcohol HL is obtained as chelate ligand. In this case the O4 group can only act as hydrogen-bond acceptor or in the absence of an appropriate hydrogen-bond donor as weakly coordinating ligand. An additional change is given by the decreased denticity of the chelate ligand. In the presence of an appropriate coligand such bidentate amino alcohol ligands are capable of supporting the common cubane-like Cu_4O_4 core structures.[30] However, also alternative motifs for the assembly of a tetranuclear core with a central μ_4-bridge have been reported for copper(II) building blocks. The most prominent is the $Cu_4(\mu_4\text{-}O)$ core with a tetrahedral assembly of copper(II) ions around a central oxoido bridge.[29] The second option is the rare case of a central μ_4-OH bridge with a square-planar assembly of the copper(II) ions leading to a $(\mu_4\text{-}OH)Cu_4O_4$ core, which as yet has only been reported for complexes supported by macrocyclic Schiff-base ligands.[24] The fact that ligand HL provides both a hydrogen-bond acceptor (O4 group) and a hydrogen-bond donor (amino group at C2) together with a rigid preset orientation of these groups given by the glucose backbone, allows for intramolecular hydrogen bonding between the {Cu(L)} building blocks in a self-complementary fashion as depicted in Figure 5. Consequently for complex **1** this leads to a $(\mu_4\text{-}OH)Cu_4O_4$ core.

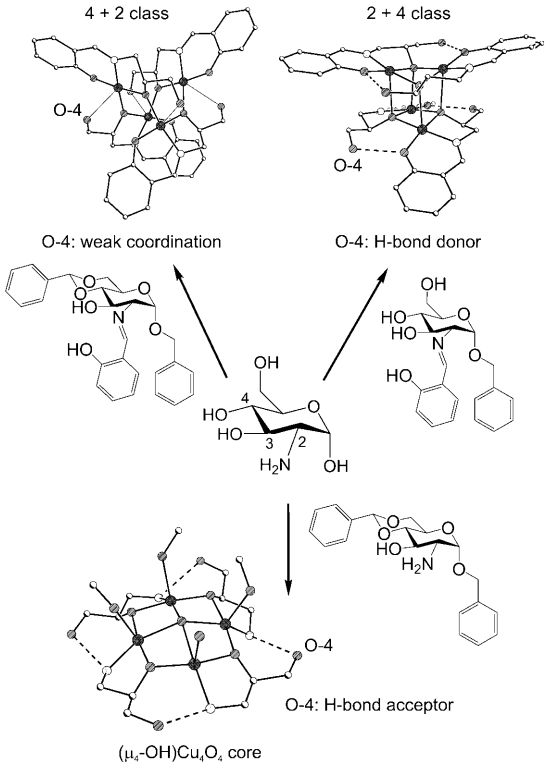

Figure 5. Structural directives for copper(II) complexes with 2-aminoglucose ligands. Variation of the 2-amino (free amine or Schiff base) and the 4-hydroxy (free or protected) functions at the backbone allows for the specific design of the self-assembly of the tetranuclear core structure (see text). Hydrogen bonds are indicated by dashed lines and weak coordinative bonds at the axial positions by thin lines. In the structural representations the non-coordinating part of the carbohydrate moiety, except for the chelate ring, is omitted for clarity.

The specific hydrogen-bonding features of the 2-aminoglucose ligand HL are ideally suited to support the rare case

of a $(\mu_3\text{-OR})_2(\mu_2\text{-OR})_2Ni_3$ core structure with an isosceles Ni_3 triangle (see Figure 6). The two ligands terminally chelating at the Ni1 and Ni2 centers seem to be of particular

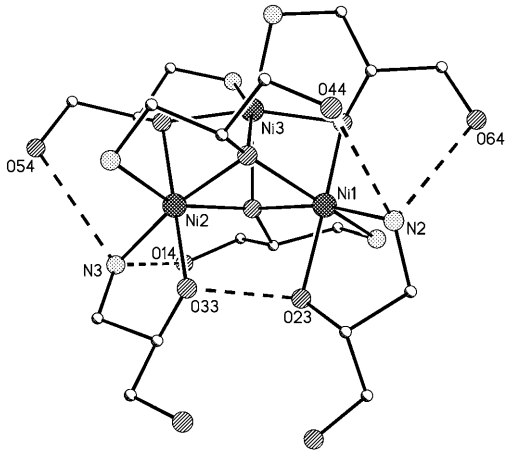

Figure 6. Hydrogen bonding for **2** supporting the trinuclear $(\mu_3\text{-OR})_2(\mu_2\text{-OR})_2Ni_3$ core structure. Hydrogen bonds are indicated by dashed lines. All atoms except the chelating part of the glucose backbone as well as the C4 and O4 atoms are omitted for clarity.

importance for the support of the core structure. Both amino groups (N2 and N3) are oriented towards one of the O4 oxygen atoms of the adjacent $\{Ni(L)_2\}$ building blocks, that is, N2 (Ni1) is hydrogen bound to O44 (Ni2) and O64 (Ni3), whereas N3 (Ni2) is hydrogen bound to O14 (Ni1) and O54 (Ni3) (for relevant distances see Figure 3). As a consequence, the two O3 oxygen atoms (O23 and O33) of these terminally bound chelate ligands are oriented towards each other which makes the relevant M-(R)O···O(R)-M fragment susceptible for protonation.[32] The resulting strong hydrogen bond with a distance of 244 pm caps the elongated basal edge of the isosceles triangle (see Table 3).

Magnetic properties: As yet neither for copper(II) complexes with a $(\mu_4\text{-OH})Cu_4O_4$ core, as observed for complex **1**, nor for nickel(II) complexes with a $(\mu_3\text{-OR})_2Ni_3$ core, as observed for complex **2**, temperature dependent magnetic measurements have been reported in the literature. For complexes **1** and **2** magnetic susceptibility measurements were performed for air-dried powdered samples in the temperature range from 2 to 300 K. The molar paramagnetic susceptibilities χ_M are corrected for the diamagnetic contributions.

The magnetic data for complex **1** are depicted in Figure 7 as temperature dependent plots of χ_M and $\chi_M T$. At room temperature a $\chi_M T$ value of $0.77\ cm^3 K mol^{-1}$ is observed. This is far from the expected spin-only value for four independent $S=1/2$ centers per molecule, which is indicative for strong antiferromagnetic interactions within the $(\mu_4\text{-OH})Cu_4O_4$ core of complex **1**. The continuous decrease of the $\chi_M T$ values with decreasing temperature further supports the presence of antiferromagnetic interactions. The low-temperature values of $\chi_M T$ are in agreement with an $S=0$ ground state for complex **1**, whereas the observed increase of the χ_M values for low temperatures are indicative for the presence of paramagnetic impurities.

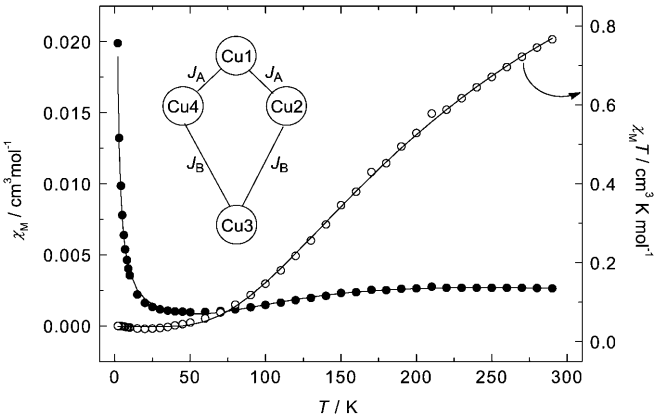

Figure 7. Plots of χ_M (●) and $\chi_M T$ (○) vs. T for **1**. The solid lines represent the calculated values (see text). The spin topology of the employed two-J model is depicted as inset.

According the rather similar intramolecular Cu···Cu distances ranging from 290 to 296 pm (see Table 1) a spin topology with equal copper(II) ions can be assumed for complex **1**. We therefore tested a one-J model with a tetragonal spin topology and equal interactions between the metal centers and a two-J model with additional diagonal interactions. Neither model yielded an acceptable fit of the experimental data. Based on the observed structural inequivalence of the four copper(II) ions of the $(\mu_4\text{-OH})Cu_4O_4$ core of complex **1** an alternative spin topology is suggested. This inequivalence is due to the variation of the apical ligands at the square-pyramidal copper(II) centers. For Cu3 this is a water ligand, whereas for the others a methanol molecule is coordinated (see Figure 1). This leads to a kite topology for the tetranuclear core which can be expressed as a two-J model given in Figure 7. The corresponding spin Hamiltonian with $J_A=J_{12}=J_{14}$ and $J_B=J_{23}=J_{34}$ is given in Equation (1).

$$\hat{\boldsymbol{H}} = -J_A(\hat{S}_1\hat{S}_2 + \hat{S}_1\hat{S}_4) - J_B(\hat{S}_2\hat{S}_3 + \hat{S}_3\hat{S}_4) + \sum_{i=1}^{4} g\beta\hat{S}_i\vec{H} \qquad (1)$$

A fit of the magnetic data of complex **1** based on the kite topology yields the parameters $g=2.122$, $J_1=-260$ and $J_2=-205\ cm^{-1}$. The graph for the best fit of the data is represented in Figure 7. Although this spin topology leads to an excellent agreement with the experimental data, the two coupling constants J_1 and J_2 can not unambiguously be assigned to J_A and J_B based on structural features. Attempts to introduce additional diagonal interactions (J_{13} and J_{24}), resulting in a four-J model, did not lead to an improvement of the fit quality. In fact, fitting of the data with this extended model indicated a dependence between the two new parameters.

These results indicate predominate interactions along the edges of the tetragonal (μ_4-OH)Cu_4O_4 core with four mixed hydroxido- and alkoxido-bridged Cu_2(μ-OH)(μ-OR) fragments. It is therefore tempting to interpret the data in terms of the well-known magnetostructural correlations described for dinuclear copper(II) complexes with either a μ-hydroxido or a μ-alkoxido bridged Cu_2O_2 core.[37] Nevertheless, taking the linear relationship established for μ-hydroxido bridges ($J=7270$–74.53α) and the very small Cu*i*-O1-Cu*j* bridging angles, ranging from 84.7 to 86.7°, strong ferromagnetic interactions would be predicted, which is in strong contradiction to the observations for complex **1**. Here it should be mentioned that the underlying unusually small Cu-O-Cu bridging angles are enforced by the μ_4-hydroxido bridged core structure, which in turn also leads to an elongation of the relevant Cu–OH distances. Moreover, a considerable distortion of the square-planar coordination geometry at all four copper centers is observed.

Instead assuming a predominate role of the μ-alkoxido bridges within the Cu_2O_2 cores, with Cu*i*-O*j*3-Cu*j* bridging angles ranging from 98.2 to 101.6°, strong antiferromagnetic interactions in the order of -200 to $-500\,cm^{-1}$ would be predicted ($J=7857$–82.1α). Although this is the correct sign, these values are still considerably too large. Nevertheless, it is well-known from dinuclear systems that a hinge distortion can considerably reduce the antiferromagnetic character of the relevant copper-copper coupling constant.[38] In fact, DFT calculations on dinuclear model systems indicate that a hinge distortion with a dihedral angle of 140° considerably reduces the antiferromagnetic coupling (up to several hundreds of wave numbers). Moreover, this effect is enhanced at about the same order of magnitude by the so-called out-of-plane distortion of the substituent on the bridging oxygen atom at an angle of 35°. Interestingly, for complex **1** similarly large distortions are observed, with dihedral angles in the order of approximately 160° and out-of-plane distortions of about 30°. Although this gives a consistent qualitative picture, the two bridges present in the Cu_2(μ-OH)(μ-OR) edge fragments may nevertheless counterbalance their effects, leading to a moderately antiferromagnetic coupling along the edges.

The χ_M and $\chi_M T$ plots of the magnetic data obtained for complex **2** are depicted in Figure 8. The molar susceptibility χ_M continuously increases with decreasing temperature without reaching a maximum in the investigated temperature range, whereas the $\chi_M T$ curve goes through a maximum at 10 K upon decreasing the temperature, indicating a ferromagnetic interaction between the nickel(II) centers within the trinuclear core. The decrease of the $\chi_M T$ values below 10 K can be attributed to zero-field splitting (ZFS) of the nickel(II) ions.[19,26]

According to the (μ_3-OR)$_2$Ni$_3$ core structure of complex **2**, representing an isosceles triangle, a two-*J* model is employed as spin topology (see Figure 8). The corresponding spin Hamiltonian with $J_A=J_{13}=J_{23}$ and $J_B=J_{12}$ is given in Equation (2) and includes ZFS for the nickel(II) centers. The latter was assumed to be equal with an approximate

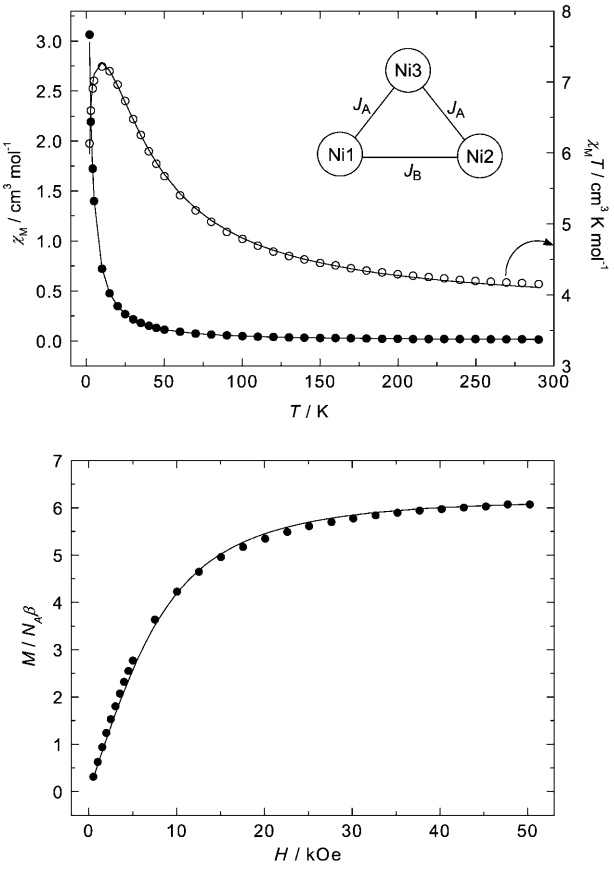

Figure 8. Top: Plots of χ_M (●) and $\chi_M T$ (○) vs T for **2**. The solid lines represent the calculated values (see text). The spin topology of the employed two-*J* model is depicted as inset. Bottom: Field-dependent magnetization for **2** at 2 K (●). The Brillouin function for $S=3$ and the appropriate g values is plotted as solid line (see text).

axial symmetry for the nickel centers Ni1 and Ni2, as both possess a similar local coordination environment (see Table 3).

$$\hat{\boldsymbol{H}} = -J_A(\hat{S}_1\hat{S}_3 + \hat{S}_2\hat{S}_3) - J_B\hat{S}_1\hat{S}_2 + \sum_{i=1}^{3} D_i[\hat{S}_{z,i}^2 - \frac{1}{3}\,S_i(S_i+1)] \sum_{i=1}^{3} g_i\beta\hat{S}_i\vec{H} \qquad (2)$$

The best fit is obtained with the parameters $g_{1,2}=2.183$, $g_3=2.247$, $J_A=16.4$, $J_B=11.0\,cm^{-1}$, $D_{1,2}=3.7$, $D_3=1.8\,cm^{-1}$ and represented in Figure 8. The observed ferromagnetic coupling within the Ni_3 core is consistent with magnetization measurements at 2 K depicted in Figure 8, which confirm a ferromagnetic $S=3$ ground state for complex **2**.

Although the effect of the ZFS is only detectable at very low temperatures, preliminary simulations of W-band ESR spectra of **2** recorded on powder samples at 10 K confirm the magnitude of the obtained values of the ZFS parameters. Moreover, these spectra even indicate a small rhombicity of the ZFS contribution. A subsequent fit of the magnetic susceptibility data including a rhombic ZFS leads to the

parameters $E_{1,2}/D_{1,2}=0.04$, $E_3/D_3=0.09$ (with $\hat{H}_{ZFS}=D[\hat{S}_z^2-\frac{1}{3}S(S+1)+E/D\ (\hat{S}_x^2-\hat{S}_y^2)]$). Nevertheless, this only leads to a marginal improvement of the fit quality, which is a fingerprint of the herewith related problem of overparametrization when a full set of ZFS parameters is used for fitting magnetic susceptibility data.

To the best of our knowledge complex **2** is the first triangular nickel(II) complex with an overall ferromagnetic interaction within the Ni_3 core. Nevertheless, for linear trinuclear complexes ferromagnetic interactions between the adjacent nickel(II) ions have been reported,[39] and date back to an early paper of Ginsberg et al.,[40] which in most cases exhibit an additional weak antiferromagnetic coupling between the two terminal nickel(II) ions. Moreover, for triangular systems generally an antiferromagnetic interaction is observed, independent of the molecular symmetry for isosceles[41] and equilateral Ni_3 triangles.[42]

However, for di-[43] and tetranuclear[44] nickel(II) complexes magnetostructural correlations have been put forward. These correlations indicate a Ni-O-Ni border line angles of about 93.5 and 99.0° for the corresponding μ_2-O and μ_3-O bridged di- and tetranuclear systems, respectively, below which a ferromagnetic interaction is observed. Interestingly, for complex **2** the Ni-(μ_2-O)-Ni angles are observed at about 89°, whereas the Ni-(μ_3-O)-Ni angles are found within range from 82 to 99°, which is consistent with the observed overall ferromagnetic interactions within the isosceles Ni_3 triangle.

Conclusion

The 2-aminoglucose ligand benzyl 2-amino-4,6-*O*-benzylidene-2-deoxy-α-D-glucopyranoside (HL) has been used to generate appropriate {Cu(L)} and {Ni(L)} building blocks which via self-assembly afford the tetranuclear μ_4-hydroxido bridged copper(II) complex **1** and the trinuclear alcoholate bridged nickel(II) complex **2**, respectively. Complex **1** represents the first example of a μ_4-hydroxido bridged copper complex not supported by a macrocyclic framework, whereas complex **2** is a rare example of a trinuclear nickel complex with a bis-μ_3-alkoxido bridged Ni_3 core structure representing an isosceles triangle. The hydrogen-bonding properties of the employed ligand, providing both hydrogen-bond donors and acceptors in a rigid preset orientation given by the glucose backbone, allows for intramolecular hydrogen bonding between the building blocks in a self-complementary fashion. In the case of copper(II) this leads to a rationale for how specific tetranuclear core structures can be generated by the choice of the appropriate functionalization of the 2-aminoglucose backbone.

Both polynuclear complexes **1** and **2** exhibit the rare coordination of the *trans*-ee-configurated donor atoms N2 and O3 of the glucose backbone which is assumed for chitosan-based metal complexes. The carbohydrate backbone adopts for both cases the stable $^4C_1$ chair conformation. The core structure of both complexes is stabilized by hydrogen bonding between the coordinating amino group of the glucose backbone and the benzyl protected oxygen atom O4 of neighboring building blocks. In the case of complex **2** a strong hydrogen bond supported by the Ni-(R)O···H-O(R)-Ni fragment is observed which is the result of an increased basicity based on the preset steric orientation of the two underlying terminal alkoxido groups.

For complex **1** antiferromagnetic interactions with a resulting $S=0$ ground state are observed, whereas for complex **2** the observed interactions are all ferromagnetic leading to an $S=3$ ground state. The nickel(II) complex **2** is the first example of a ferromagnetically coupled trinuclear nickel(II) complex. The magnetic interactions for both complexes can be interpreted in terms of superexchange via the involved oxygen bridges. Consequently, the steric presettings given by the glucose backbone of the ligand have a strong influence on the observed magnetic interactions.

Experimental Section

Physical measurements: Melting points are given uncorrected and were determined via a VEB Analytik Dresden HMK 72/41555. Thermogravimetric analyses (TGA) for powdered samples were performed on a NETZSCH STA409PC Luxx apparatus under a constant flow of nitrogen ranging from room temperature up to 1000°C with a heating rate of 1°C min^{-1}. Infrared and Raman spectra were recorded on a BRUKER IFS 55 EQUINOX spectrometer. UV/Vis spectra were recorded on a VARIAN CARY 5000 UV/Vis-NIR-spectrometer. Mass spectra were measured on a Bruker MAT SSQ 710 spectrometer. Elemental analyses were determined on a LECO CHNS/932 Analyser and a VARIO EL III. Magnetic susceptibilities were obtained from a powdered sample of **1** and from a paraffin-triturated sample of **2** using a Quantum-Design MPMSR-5S SQUID magnetometer equipped with a 5 Tesla magnet in the range from 300 to 2 K with an applied magnetic field of 5000 Oe (for details see ref. [45]). The experimental magnetic susceptibility data were fitted using the program package julX version 1.3 which allows spin-Hamiltonian simulations of the data by a full-matrix diagonalization approach and includes the treatment of paramagnetic impurities in the fitting procedure.[46]

Syntheses: The ligand benzyl 2-amino-4,6-*O*-benzylidene-2-deoxy-α-D-glucopyranoside (HL) was synthesized starting from *N*-acetyl-α-D-glucopyranosamine according to the published procedures.[23] All chemicals were purchased from commercial suppliers and used without further purification.

CAUTION: In general, perchlorate salts of metal complexes with organic ligands are potentially explosive. While the present complex has not proved to be shock sensitive, only small quantities should be prepared and great care is recommended.

[(μ_4-OH)Cu_4(L)$_4$(MeOH)$_3$(H_2O)](ClO_4)$_3$ (1): A solution of Cu(ClO_4)$_2$·6H_2O (519 mg, 1.40 mmol) in methanol (6.6 mL) was added to a solution of the ligand HL (500 mg, 1.40 mmol) in chloroform (20 mL) at room temperature. After 7 d of slow evaporation complex **1** was obtained as blue prismatic crystals of **1**·2.7MeOH which were suitable for X-ray diffraction. The crystals were isolated, washed with a small amount of methanol, and dried in air. Yield: 198 mg (28%). Decomposition interval = 191–222°C; IR (KBr): $\tilde{\nu}$ = 3448 (br, ν O–H), 3326 and 3260 (m, ν N–H), 3169, 3067, and 3033 (w, ν C–H arom.), 2934 and 2911 (w, ν_{as} CH_2), 2874 (w, ν_s CH_2), 1617 (w, ν C=C), 1456 (m, δ CH_2), 1385 (m), 1200 (w, ν C–O), 1132, 1122, and 1093 (vs, ν Cl–O and C–O), 1069, 1055, and 1026 (vs, ν C–O), 990 (s), 927 (m), 764 (m), 737 (m), 701 (s), 668 (m), 624 (m) cm^{-1}; Raman (solid): $\tilde{\nu}$ = 3066 (s, ν C–H arom.), 2943 (m, ν_{as} CH_2), 2875 (m, ν_s CH_2), 1606 (m, ν C=C), 1028 (w, ν C–O), 1003 (s, ν C–O), 930 (m) cm^{-1}; UV/Vis ($CHCl_3$): λ_{max} (ε) = 278 (11.100), 696 nm

($264\,M^{-1}\,cm^{-1}$); MS (micro-ESI in EtOH): *m/z* (%): 380 (100) $[L+Na]^+$, 777 (8) $[\{Cu(L)_2\}+H]^+$, 840 (16) $[\{Cu_2(L)_2\}+H]^+$, 1195 (5) $[\{Cu_2(L)_3\}]^+$; elemental analysis calcd (%) for **1**·2.7 MeOH, $C_{85.7}H_{113.8}Cl_3Cu_4N_4O_{39.7}$ (2195.72): C 46.88, H 5.22, N 2.55; found: C 45.27, H 4.74, N 2.53.

$[Ni_3(L)_5(HL)]NO_3$ (2): Under vigorous stirring a solution of $Ni(NO_3)_2$·$6H_2O$ (82 mg, 0.28 mmol) in methanol (5 mL) was added to a suspension of the ligand HL (200 mg, 0.56 mmol) in methanol (10 mL) at room temperature. The addition of an aqueous potassium hydroxide solution (283 μL, 1.98 M) led to a pale green solution. After three weeks of slow evaporation complex **2** was obtained as green prisms of **2**·3.25 MeOH·0.75 H_2O which were suitable for X-ray crystallography. The crystals were isolated, washed with a small amount of methanol, and dried in air. Yield: 69 mg (31 %). Decomposition interval = 251–264 °C; IR (KBr): $\tilde{\nu}$ = 3435 (br, ν O–H), 3375, 3342, and 3284 (m, ν N–H), 3064 and 3033 (w, ν C–H arom.), 2929 and 2911 (w, ν_{as} CH_2), 2862 (m, ν_s CH_2), 1608 and 1498 (w, ν C=C), 1455 (m, δ CH_2), 1384 (s, ν N=O), 1216 and 1191 (m, ν C–O), 1138 (s, ν C–O), 1090, 1072, 1024, and 984 (vs, ν C–O), 918 (m), 876 (w), 756 (m), 734 (m), 698 (s), 678 (w), 659 (w) cm^{-1}; UV/Vis ($CHCl_3$): λ_{max} (ε) = 381 (67), 643 (18), 1131 ($26\,M^{-1}\,cm^{-1}$); MS (micro-ESI in $CHCl_3$/MeOH): *m/z* (%): 772 (100) $[\{Ni(L)_2\}+H]^+$, 1544 (12) $[\{Ni_2(L)_4\}+H]^+$, 1958 (56) $[\{Ni_3(L)_5\}]^+$, 2315 (2) $[\{Ni_3(L)_6\}+H]^+$; elemental analysis calcd (%) for **2**·3.25 MeOH·0.75 H_2O, $C_{123.25}H_{147.5}N_7Ni_3O_{37}$ (2495.11): C 59.33, H 5.87, N 3.93; found: C 59.58, H 5.68, N 3.89.

X-ray structure determination: Single crystals were selected while still covered with mother liquor under a polarizing microscope and fixed on fine glass fibers. Single crystal X-ray measurements were carried out on a Nonius Kappa CCD diffractometer using graphite monochromated $Mo_{K\alpha}$ radiation (λ = 71.073 pm). The structures were solved by direct methods with SHELXS-97 and were full-matrix least-squares refined against F^2 using SHELXL-97.[47] The program XP (SIEMENS Analytical X-ray Instruments, Inc.) was used for structure representations. Hydrogen atoms were calculated and treated as riding atoms with fixed thermal parameters. For **1**·2.7 MeOH anisotropic thermal parameters were used for all non-hydrogen atoms except for the disordered benzyl substituents. The perchlorate ion Cl1P, located in the cavity below the Cu_4 plane which is opposite to the μ_4-OH group, is disordered with an occupation factor of 0.5 at two crystallographic positions. This is consistent with the flexibility of the hydrogen bonding interactions through the four amino N-H donors within the cavity. For Cl2P no disorder is observed, whereas the perchlorate ion Cl3P is highly disordered. This again also reflects in the spacial flexibility of the crystallographic cavity given by possible hydrogen-bonding interactions. In fact this perchlorate ion is disordered at four crystallographic positions (occupations: 0.4, 0.3, 0.15, 0.15). When the two more probable of these positions are filled an additional methanol molecule with an occupation factor of 0.7 is present in its vicinity. For **2**·3.25 MeOH·0.75 H_2O anisotropic thermal parameters were used for all non-hydrogen atoms except for the disordered benzyl substituents, the disordered water molecules, and some of the partially occupied methanol molecules. Details of the data collection and refinement procedure are summarized in Table 4.

CCDC 682760, 682761 contain the supplementary crystallographic data for this paper. These data can be obtained free of charge from The Cambridge Crystallographic Data Centre via www.ccdc.cam.ac.uk/data_request/cif.

Table 4. Crystallographic data for **1**·2.7 MeOH and **2**·3.25 MeOH·0.75 H_2O.

formula	$C_{85.7}H_{113.8}Cl_3Cu_4N_4O_{39.7}$	$C_{123.25}H_{147.5}N_7Ni_3O_{37}$
M_r [g mol^{-1}]	2195.72	2495.11
T [K]	183(2)	183(2)
crystal size [mm]	0.85 × 0.65 × 0.45	0.50 × 0.50 × 0.50
crystal system	monoclinic	monoclinic
space group	$P2_1$	$P2_1$
a [pm]	1620.1(3)	1552.50(3)
b [pm]	1932.0(4)	1650.06(4)
c [pm]	1689.0(3)	2556.08(4)
β [°]	112.61(3)	105.8890(10)
V [nm^3]	4.8803(17)	6.2978(2)
Z	2	2
ρ_{calcd} [g cm^{-3}]	1.494	1.316
μ [mm^{-1}]	1.032	0.526
θ_{min}, θ_{max} [°]	2.44–27.49	2.78–27.49
unique data	20946	24506
data with $I > 2\sigma(I)$	15547	19301
no. of parameters	1339	1560
goodness-of-fit on F^2	1.025	1.019
$wR2$ (all data, F^2)	0.1234	0.1342
$R1$ ($I > 2\sigma(I)$)	0.0530	0.0530
flack parameter	0.001(11)	−0.008(9)

Acknowledgements

This work was financially supported by the "Deutsche Forschungsgemeinschaft" (SFB 436 "Metal Mediated Reactions Modeled after Nature" and SPP 1137 "Molecular Magnetism"). E.T.S. gratefully acknowledges financial support by the Graduiertenförderung of the Freistaat Thüringen and the Carl-Zeiss Stiftung. We also thank the Marie-Curie training site LAboratory for Molecular Magnetism (LAMM) in Florence, Italy.

[1] J. F. Kennedy, C. A. White, *Bioactive Carbohydrates in Chemistry, Biochemistry and Biology*, Wiley, New York **1983**.

[2] a) H. Häusler, A. E. Stütz, *Top. Curr. Chem.* **2001**, *215*, 77–114; b) X. He, G. Agnihotri, H.-W. Liu, *Chem. Rev.* **2000**, *100*, 4615–4661; c) S. H. Bhosale, M. B. Rao, V. V. Deshpande, *Microbiol. Rev.* **1996**, *60*, 280–300; d) R. W. Gracy, E. A. Noltmann, *J. Biol. Chem.* **1968**, *243*, 4109–4116; e) K. D. Hardman, R. C. Agarwal, M. J. Freiser, *J. Mol. Biol.* **1982**, *157*, 69–86; f) R. L. Root, J. R. Durrwachter, C.-H. Wong, *J. Am. Chem. Soc.* **1985**, *107*, 2997–2999; g) G. K. Farber, A. Glasfeld, G. Tiraby, D. Ringe, G. A. Petsko, *Biochemistry* **1989**, *28*, 7289–7297; h) J. Jenkins, J. Janin, F. Rey, M. Chiadmi, H. van Tilbeurgh, I. Lasters, M. De Maeyer, D. Van Belle, S. J. Wodak, M. Lauwereys, P. Stanssens, N. T. Mrabet, J. Snauwaert, G. Matthyssens, A.-M. Lambeir, *Biochemistry* **1992**, *31*, 5449–5458; i) Y. Zhang, J.-Y. Liang, S. Huang, H. Ke, W. N. Lipscomb, *Biochemistry* **1993**, *32*, 1844–1857; j) A. Lavie, K. N. Allen, G. A. Petsko, D. Ringe, *Biochemistry* **1994**, *33*, 5469–5480; k) K. K.-S. Ng, W. I. Weis, *Biochemistry* **1997**, *36*, 979–988.

[3] S. Yano, Y. Mikata, *Bull. Chem. Soc. Jpn.* **2002**, *75*, 2097–2113.

[4] a) Y. E. Alexeev, I. S. Vasilchenko, B. I. Kharisov, L. M. Blanco, A. D. Garnovskii, Y. A. Zhdanov, *J. Coord. Chem.* **2004**, *57*, 1447–1517; b) D. Steinborn, H. Junicke, *Chem. Rev.* **2000**, *100*, 4283–4317; c) B. Gyurcsik, L. Nagy, *Coord. Chem. Rev.* **2000**, *203*, 81–149; d) S. Yano, *Coord. Chem. Rev.* **1988**, *92*, 113–156.

[5] R. H. Holm, P. Kennepohl, E. I. Solomon, *Chem. Rev.* **1996**, *96*, 2239–2314.

[6] a) O. Kahn, *Molecular Magnetism*, VCH, Weinheim **1993**; b) R. E. P. Winpenny, *Adv. Inorg. Chem.* **2001**, *52*, 1–111.

[7] a) P. Klüfers, O. Krotz, M. Oßberger, *Eur. J. Inorg. Chem.* **2002**, 1919–1923; b) P. Klüfers, T. Kunte, *Eur. J. Inorg. Chem.* **2002**, 1285–1289; c) P. Klüfers, T. Kunte, *Angew. Chem.* **2001**, *113*, 4356–4358; *Angew. Chem. Int. Ed.* **2001**, *40*, 4210–4212; d) N. Habermann, G. Jung, M. Klaassen, P. Klüfers, *Chem. Ber.* **1992**, *125*, 809–814.

[8] T. Tanase, H. Inukai, T. Onaka, M. Kato, S. Yano, S. J. Lippard, *Inorg. Chem.* **2001**, *40*, 3943–3953.

[9] a) T. Tanase, Y. Yasuda, T. Onaka, S. Yano, *J. Chem. Soc. Dalton Trans.* **1998**, 345–352; b) T. Tanase, M. Nakagoshi, A. Teratani, M. Kato, Y. Yamamoto, S. Yano, *Inorg. Chem.* **1994**, *33*, 5–6.

[10] a) Y. Mikata, Y. Shinohara, K. Yoneda, Y. Nakamura, K. Esaki, M. Tanahashi, I. Brudziñska, S. Hirohara, M. Yokoyama, K. Mogami, T. Tanase, T. Kitayama, K. Takashiba, K. Nabeshima, R. Takagi, M.

Takatani, T. Okamoto, I. Kinoshita, M. Doe, A. Hamazawa, M. Morita, F. Nishida, T. Sakakibara, C. Orvig, S. Yano, *J. Org. Chem.* **2001**, *66*, 3783–3789; b) Y. Mikata, Y. Sugai, S. Yano, *Inorg. Chem.* **2004**, *43*, 4778–4780; c) T. Storr, Y. Sugai, C. A. Barta, Y. Mikata, M. J. Adam, S. Yano, C. Orvig, *Inorg. Chem.* **2005**, *44*, 2698–2705; d) T. Storr, M. Obata, C. L. Fisher, S. R. Bayly, D. E. Green, I. Brudziñska, Y. Mikata, B. O. Patrick, M. J. Adam, S. Yano, C. Orvig, *Chem. Eur. J.* **2005**, *11*, 195–203; e) Y. Mikata, Y. Sugai, M. Obata, M. Harada, S. Yano, *Inorg. Chem.* **2006**, *45*, 1543–1551.

[11] J. Becher, I. Seidel, W. Plass, D. Klemm, *Tetrahedron* **2006**, *62*, 5675–5681.

[12] a) M. E. Cucciolito, R. Del Litto, G. Roviello, F. Ruffo, *J. Mol. Catal. A* **2005**, *236*, 176–181; b) J. C. Irvine, J. C. Earl, *J. Chem. Soc.* **1922**, *121*, 2376–2381.

[13] a) A. K. Sah, C. P. Rao, P. K. Saarenketo, E. K. Wegelius, E. Kolehmainen, K. Rissanen, *Eur. J. Inorg. Chem.* **2001**, 2773–2781; b) J. Zhao, X. Zhou, A. M. Santos, E. Herdtweck, C. C. Romão, F. E. Kühn, *Dalton Trans.* **2003**, 3736–3742.

[14] a) R. Wegner, M. Gottschaldt, H. Görls, E.-G. Jäger, D. Klemm, *Angew. Chem.* **2000**, *112*, 608–612; *Angew. Chem. Int. Ed.* **2000**, *39*, 595–599; b) R. Wegner, M. Gottschaldt, H. Görls, E.-G. Jäger, D. Klemm, *Chem. Eur. J.* **2001**, *7*, 2143–2157; c) A. K. Sah, C. P. Rao, P. K. Saarenketo, K. Rissanen, G. A. van Albada, J. Reedijk, *Chem. Lett.* **2002**, *31*, 348–349; d) A. K. Sah, T. Tanase, *Chem. Commun.* **2005**, 5980–5981; e) A. K. Sah, M. Kato, T. Tanase, *Chem. Commun.* **2005**, 675–677; f) A. Roth, J. Becher, C. Herrmann, H. Görls, G. Vaughan, M. Reiher, D. Klemm, W. Plass, *Inorg. Chem.* **2006**, *45*, 10066–10076.

[15] A. Fragoso, M. L. Kahn, A. Castiñeiras, J.-P. Sutter, O. Kahn, R. Cao, *Chem. Commun.* **2000**, 1547–1548.

[16] A. K. Sah, T. Tanase, M. Mikuriya, *Inorg. Chem.* **2006**, *45*, 2083–2092.

[17] A. Burkhardt, E. T. Spielberg, H. Görls, W. Plass, *Inorg. Chem.* **2008**, *47*, 2485–2493.

[18] A. Burkhardt, A. Buchholz, H. Görls, W. Plass, *Eur. J. Inorg. Chem.* **2006**, 3400–3406.

[19] A. Burkhardt, W. Plass, *Inorg. Chem. Commun.* **2008**, *11*, 303–306.

[20] A. Burkhardt, H. Görls, W. Plass, *Carbohydr. Res.* **2008**, *343*, 1266–1277.

[21] a) S. Yano, M. Doi, S. Tamakoshi, W. Mori, M. Mikuriya, A. Ichimura, I. Kinoshita, Y. Yamamoto, T. Tanase, *Chem. Commun.* **1997**, 997–998; b) T. Tanase, S. Tamakoshi, M. Doi, M. Mikuriya, H. Sakurai, S. Yano, *Inorg. Chem.* **2000**, *39*, 692–704.

[22] a) T. Tanase, K. Kurihara, S. Yano, K. Kobayashi, T. Sakurai, S. Yoshikawa, *J. Chem. Soc. Chem. Commun.* **1985**, 1562–1563; b) T. Tanase, K. Kurihara, S. Yano, K. Kobayashi, T. Sakurai, S. Yoshikawa, M. Hidai, *Inorg. Chem.* **1987**, *26*, 3134–3139; c) J. Burger, C. Gack, P. Klüfers, *Angew. Chem.* **1995**, *107*, 2950–2951; *Angew. Chem. Int. Ed. Engl.* **1995**, *34*, 2647–2649; d) T. Tanase, T. Onaka, M. Nakagoshi, I. Kinoshita, K. Shibata, M. Doe, J. Fujii, S. Yano, *Chem. Commun.* **1997**, 2115–2116; e) T. Tanase, T. Onaka, M. Nakagoshi, I. Kinoshita, K. Shibata, M. Doe, J. Fujii, S. Yano, *Inorg. Chem.* **1999**, *38*, 3150–3159.

[23] a) P. H. Gross, R. W. Jeanloz, *J. Org. Chem.* **1967**, *32*, 2759–2763; b) Z. Györgydeák, *Liebigs Ann. Chem.* **1991**, 1291–1300; c) A. Burkhardt, A. Buchholz, H. Görls, W. Plass, *Acta Crystallogr. Sect. E* **2007**, *E63*, o2527–o2529.

[24] a) V. McKee, S. S. Tandon, *J. Chem. Soc. Dalton Trans.* **1991**, 221–230; b) V. McKee, S. S. Tandon, *J. Chem. Soc. Chem. Commun.* **1988**, 385–387.

[25] V. Lozan, A. Buchholz, W. Plass, B. Kersting, *Chem. Eur. J.* **2007**, *13*, 7305–7316.

[26] A. Roth, A. Buchholz, M. Rudolph, E. Schütze, E. Kothe, W. Plass, *Chem. Eur. J.* **2008**, *14*, 1571–1583.

[27] W. Plass, H. P. Yozgatli, *Z. Anorg. Allg. Chem.* **2003**, *14*, 65–70.

[28] I. D. Brown, D. Altermatt, *Acta Crystallogr. Sect. B* **1985**, *41*, 244–247.

[29] a) A. M. Kirillov, M. N. Kopylovich, M. V. Kirillova, M. Haukka, M. F. C. G. da Silva, A. J. L. Pombeiro, *Angew. Chem.* **2005**, *117*, 4419–4423; *Angew. Chem. Int. Ed.* **2005**, *44*, 4345–4349; b) M. Bera, W. T. Wong, G. Aromi, J. Ribas, D. Ray, *Inorg. Chem.* **2004**, *43*, 4787–4789; c) S. Mukherjee, T. Weyhermüller, E. Bothe, K. Wieghardt, P. Chaudhuri, *Eur. J. Inorg. Chem.* **2003**, 863–875; d) J. Reim, R. Werner, W. Haase, B. Krebs, *Chem. Eur. J.* **1998**, *4*, 289–298.

[30] E. Ruiz, A. Rodríguez-Fortea, P. Alemany, S. Alvarez, *Polyhedron* **2001**, *20*, 1323–1327.

[31] T. C. Higgs, C. J. Carrano, *Inorg. Chem.* **1997**, *36*, 298–306.

[32] W. Plass, A. Pohlmann, J. Rautengarten, *Angew. Chem.* **2001**, *113*, 4333–4336; *Angew. Chem. Int. Ed.* **2001**, *40*, 4207–4210.

[33] A. Yuchi, H. Murakami, M. Shiro, H. Wada, G. Nakagawa, *Bull. Chem. Soc. Jpn.* **1992**, *65*, 3362–3373.

[34] E. Ilina, V. G. Kessler, *Polyhedron* **2005**, *24*, 3052–3056.

[35] A. K. Sah, C. P. Rao, P. K. Saarenketo, K. Rissanen, *Chem. Lett.* **2001**, *11*, 1296–1297.

[36] a) L. Merz, W. Haase, *J. Chem. Soc. Dalton Trans.* **1978**, 1594–1598; b) R. Mergehenn, W. Haase, *Acta Crystallogr. Sect. B* **1977**, *33*, 2734–2739; c) J. Tercero, E. Ruiz, S. Alvarez, A. Rodríguez-Fortea, P. Alemany, *J. Mater. Chem.* **2006**, *16*, 2729–2735.

[37] F. Tuna, L. Patron, Y. Journaux, M. Andruh, W. Plass, J.-C. Trombe, *J. Chem. Soc. Dalton Trans.* **1999**, 539–545.

[38] a) M. F. Charlot, O. Kahn, S. Jeannin, Y. Jeannin, *Inorg. Chem.* **1980**, *19*, 1410–1411; b) E. Ruiz, P. Alemany, S. Alvarez, J. Cano, *Inorg. Chem.* **1997**, *36*, 3683–3688; c) E. Ruiz, P. Alemany, S. Alvarez, J. Cano, *J. Am. Chem. Soc.* **1997**, *119*, 1297–1303.

[39] A. K. Sharma, F. Lloret, R. Mukherjee, *Inorg. Chem.* **2007**, *46*, 5128–5130; and references therein.

[40] A. P. Ginsberg, R. L. Martin, R. C. Sherwood, *Inorg. Chem.* **1968**, *7*, 932–936.

[41] a) T. Weyhermüller, R. Wagner, S. Khanra, P. Chaudhuri, *Dalton Trans.* **2005**, 2539–2546; b) H. Adams, D. E. Fenton, L. R. Cummings, P. E. McHugh, M. Ohba, H. Okawa, H. Sakiyama, T. Shiga, *Inorg. Chim. Acta* **2004**, *357*, 3648–3656; c) A. Escuer, M. S. El Fallah, S. B. Kumar, F. Mautner, R. Vicente, *Polyhedron* **1998**, *8*, 377–381; d) V. V. Pavlishchuk, S. V. Kolotilov, A. W. Addison, M. J. Prushan, R. J. Butcher, L. K. Thompson, *Inorg. Chem.* **1999**, *38*, 1759–1766; e) A. Escuer, R. Vicente, S. B. Kumar, X. Solans, M. Font-Bardia, A. Caneschi, *Inorg. Chem.* **1996**, *35*, 3094–3098.

[42] a) A. E. Ion, E. T. Spielberg, H. Görls, W. Plass, *Inorg. Chim. Acta* **2007**, *360*, 3925–3931; b) L. K. Thompson, V. Niel, H. Grove, D. O. Miller, M. J. Newlands, P. H. Bird, W. A. Wickramasinghe, A. B. P. Lever, *Polyhedron* **2004**, *23*, 1175–1184.

[43] X.-H. Bu, M. Du, L. Zhang, D.-Z. Liao, J.-K. Tang, R.-H. Zhang, M. Shionoya, *J. Chem. Soc. Dalton Trans.* **2001**, 593–598.

[44] a) M. A. Halcrow, J.-S. Sun, J. C. Huffman, G. Christou, *Inorg. Chem.* **1995**, *34*, 4167–4177; b) J. M. Clemente-Juan, B. Chansou, B. Donnadieu, J.-P. Tuchagues, *Inorg. Chem.* **2000**, *39*, 5515–5519.

[45] a) W. Plass, *Angew. Chem.* **1996**, *108*, 699–703; *Angew. Chem. Int. Ed. Engl.* **1996**, *35*, 627–631; b) W. Plass, *Inorg. Chem.* **1997**, *36*, 2200–2205.

[46] E. Bill, Program package julX Version 1.3, MPI for Bioinorganic Chemistry, Mühlheim/Ruhr (Germany), **2007**.

[47] G. M. Sheldrick, SHELXS-97 and SHELXL-97, University of Göttingen, Göttingen (Germany), **1997**.

Received: April 8, 2008
Revised: August 14, 2008
Published online: December 19, 2008

